BULLETIN OF THE EARTHQUAKE
RESEARCH INSTITUTE
Vol. 57 (1982), pp. 273-302

14. *Numerical Analysis of Layered Convection —Marginal Stability and Finite Amplitude Analyses—*

By Satoru HONDA,
Earthquake Research Institue.
(Received April 30, 1982)

Abstract

A study of infinitesimal and finite amplitude convections in two layered immiscible fluids heated from below is presented. In the marginal stability analysis, changing the parameters, e.g. geometrical constraints and viscosity, we find that there are two modes of coupling between the upper and lower convecting fiuids as was previously pointed out by UKAJI and SAWADA (1970 a, b, 1971). The first is the 'mechanical coupling' in which the horizontal component of the velocity near the interface between two fluids runs in the same direction. The second is the 'thermal coupling' in which the horizontal component of the velocity near the interface runs in the opposite direction. If one of the two fluids becomes more unstable, it drags the other. This is clearly a modified 'mechanical coupling' mode which we tentatively call the 'dragging mode'. The thermal coupling may be a more excited state than the 'mechanical coupling'. Several stability curves obtained by the analysis can be roughly explained in terms of the instability in each layer. In the study of the finite amplitude convection with the infinite Prandtl number, we calculate the Nusseldt number, temperature, stream function and vorticity for various Rayleigh numbers for three kinds of models. The calculated Nusseldt number—Rayleigh number relations are explained by a simple parameterized analysis in spite of the non-linear nature of the problem. This parameterization is possible because the interface between the two immiscible fluids is a plane of almost zero shear stress and the temperature at the interface is nearly constant. Thus, the efficiency of the heat transport can be estimated as follows;

1) calculate 'local' Rayleigh numbers defined for each layer.
2) assume that the Nusseldt number—'local' Rayleigh number relation for each layer is the same as that of 'one' layer.
3) formulate the equation of continuity of the heat flux at the interface.

As a result of procedure (3), we can obtain the temperature at the interface and also the total heat flux flowing through the convection system. Well developed thermal boundary layers are formed at the top and bottom surfaces and the interface, when appropriately defined

Rayleigh number many times exceeds the critical Rayleigh number. All the flow fields obtained in the study of the finite amplitude convection are of the 'mechanical coupling' mode. This mode may exist in the mantle, if the mantle consists of several independently convecting layers.

1. Introduction

There are two main kinds of models of the covection in the mantle. One is the 'whole mantle convection' model having the cell size of mantle-wide scale (DAVIES, 1977; ELSASSER *et al.*, 1978), and the other is the 'layered convection' model in which the mantle is divided radially into several convecting systems between which no or only a small mass exchange exists (MCKENZIE and WEISS, 1975, RICHTER, 1979). A distinction between these two models may be found from observations such as heat flow, gravity field, world-wide plate motions and geochemical evidence. Unfortunately, as discussed frequently, because plates screen the information from the under-plate structures, inverse problems of revealing the pattern of the convection in the mantle from the surface data is difficult to solve. For example, the first order heat flow distribution in the oceanic area can be explained by the simple plate model in which a plate cools as it moves away from the ridge (SCLATER *et al.*, 1980), so that we cannot easily find the thermal anomalies which may be related to the flow beneath the plate.

Previous arguments on the convection in the mantle were mainly based on the theory and experiment of 'one' layered convection (e.g. MCKENZIE *et al.*, 1974; ROSSBY, 1969). The main results concerning the simple Rayleign-Benard type convection (i.e. constant physical properties, heated from below etc.) obtained up until now may be summarized as follows:

(1) Convection (or instability) sets in only when the appropriately defined Rayleigh number becomes equal to or greater than a certain critical Rayleigh number of about 1000 which is weakly dependent on the boundary conditions (CHANDRASEKHR, 1961).

(2) The effciency of heat transport is measured or represented by a Nusseldt number (the ratio of the total heat flux carried by the convection and conduction to the hypothetical heat flux carried when only the conduction is assumed). If the Rayleigh number is much greater than the critical Rayleigh number and the Prandtl number is also many times larger than one, the relation between the Nusseldt number (Nu) and the Rayleigh number (Ra) is roughly expressed as,

$$Nu=b(Ra/Rc)^a \qquad (1),$$

where a and b are constants of about 0.3 and 1 respectively and Rc is the critical Rayleigh number. This formulation has been confirmed by both experiment (ROSSBY, 1969) and numerical simulations (MOORE and WEISS, 1973).

(3) When the Rayleigh number is large enough, there appears a boundary layer where the temperature varies rapidly, and a viscous core where a nearly constant temperature (or adiabatic temperature gradient, if the compressibility cannot be neglected; JARVIS and MCKENZIE, 1979) is attained (TURCOTTE and OXBURGH, 1969).

(4) The above simple formula for Nu and Ra (equation (1)) can be derived from the boundary layer theory (TURCOTTE and OXBURGH, 1969; MCKENZIE *et al.*, 1974).

(5) The aspect ratio of the convection cell is nearly one. This is one of the reasons for rejecting the simple correspondence between the plate system and the convection (especially so when the convection is supposed to be confined in the upper mantle).

If the mantle is divided into a few convection systems radially (RICHTER, 1979; ANDERSON, 1980), there arises a situation different from that of 'one' layered convection because of the thermal and viscous coupling between convections. In this study, to investigate these problems, we first conduct a marginal stability analysis and secondly we model the 'pseudo' (the meaning of this terminology will be given in section 4 of this paper) two-layered convection. We will show that, if the convection becomes highly vigorous, a simple parameterization in the sense of superposition is applicable in spite of the non-linearity of the problem. To understand the dependence of the convection on specific parameters (e.g. viscosity, geometry) we construct a fairly generalized model instead of attempting to make the model as real as possible. Results obtained by our approach will be useful, when, in the future, we will have determined the parameters which are not well constrained now. Also, we may be able to use the results in the study of the earth's thermal history by the 'parameterized' convection approach (MCKENZIE and WEISS, 1975; SHARPE and PELTIER, 1979).

2. Marginal Stability Analysis

The model which we are considering is illustrated schematically in Fig. 1, which is modified from ZEREN and REYNOLDS (1972). The convection system consists of two immiscible fluids, distinguished by subscripts 1 and 2 (1=upper, 2=lower), having constant physical properties. When the upper layer is initially denser than the lower, this system, known as Rayleigh-Taylor instability, is intrinsically unstable. However, in this study,

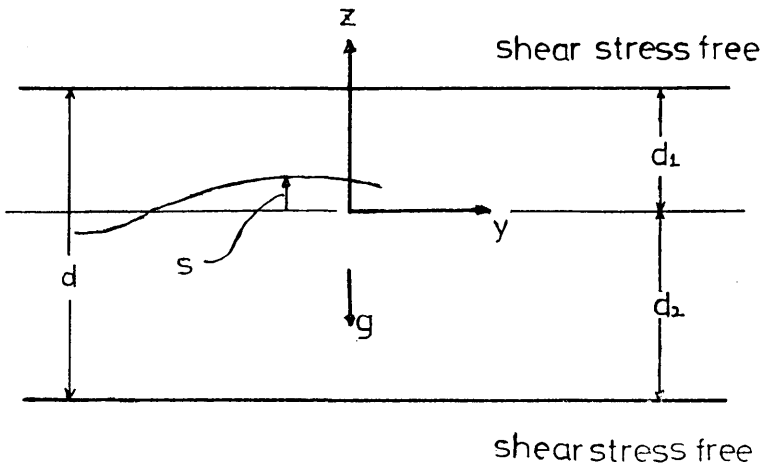

Fig. 1. Schematic view of the two-immiscible fluids model. The system is initially stably stratified (i.e. $\rho_2>\rho_1$). The top and bottom surfaces are both shear stress free.

we consider the case where the lower layer is denser than the upper so that the system is initially stable. This problem was partly solved by SMITH (1966), ZEREN and REYNOLDS (1972), UKAJI and SAWADA (1970a, b, 1971) and RICHTER and JOHNSON (1974). SMITH (1966) and ZEREN and REYNOLDS (1972) studied the same problem as the present one including the effect of surface tension. Because their main interest was on the surface tension, their results are not directly applicable to the convection in the mantle on which our main interest lies. Although UKAJI and SAWADA's studies (1970a, b, 1971) were only sporadically reported, they contain some important results on the coupling between two fluids as will be described later. RICHTER and JOHNSON's work (1974) is the first study, as far as we know, to apply the layered convection model to the earth's mantle, but only the symmetric ($d_1=d_2$) and constant viscosity cases were investigated. We intend to extend their work, and show some important aspects of the interaction of the two convecting fluids.

Important symbols used in this study are listed and explained in Appendix 1. The basic equations which govern the imcompressible Boussinesq fluid motion are those on the conservation of mass, momentum and energy, i.e.

$$div\cdot \boldsymbol{u}_i=0, \tag{2a}$$

$$\rho_i\frac{D\boldsymbol{u}_i}{Dt}=-\nabla p_i+\nu_i\Delta^2\boldsymbol{u}_i+\alpha_i\theta_i\boldsymbol{g}, \tag{2b}$$

$$\frac{DT_i}{Dt}=\kappa_i\nabla^2T_i, \qquad (i=1, 2) \tag{2c}$$

where the constitutive equation for Newtonian fluid and Boussinesq approximation are assumed. In these equations, $\boldsymbol{u}_i$, ρ_i, D/Dt, p_i, ν_i, α_i, θ_i, $\boldsymbol{g}$, T_i, κ_i are velocity vector, density, material derivatives, pressure, kinematic viscosity, coefficient of volume thermal expansion, perturbed temperature, gravity, temperature and thermal diffusivity. Complementary conditions to these basic equations are boundary conditions at $z=d_1$, $-d_2$ and 0. They are, at the upper and lower surfaces, (1) zero vertical velocity, (2) constant temperature, (3) zero shear stress, and at the interface between two fluids, continuity of (4) velocity, (5) temperature, (6) heat flux, (7) shear stress and (8) normal stress. One other special condition at the interface is the kinematic condition, that is, the deformation velocity of the interface is equal to the vertical component of the velocity of each fluid.

The essence of the usual marginal stability analysis is that the perturbations caused by the instability is small and all the cross products of them can be neglected. Also we assume that the perturbations are expressed as

$$w=W(z)\exp(ik_x x+ik_y y+nt), \tag{3}$$

where w and W are the perturbations of vertical component of velocity and amplitude. After following the usual techniques described in CHANDRASEKHAR's classic work (1961), we can eliminate the variable except for w by the combination of equations (2a) and (2b). The resultant equation is a six order ordinary differential equation of W with regard to z. As a result, W can be expressed by a linear combination of six eigen functions. This implies that twelve constants are undetermined (six for the upper layer and six for the lower layer). In addition, there is one additional constant related to the deformation of the interface. Combined with the boundary conditions, we can obtain thirteen linear equations for thirteen constants. To get non zero thirteen constants, we must require that the determinant derived from the coefficient matrix (13×13) of thirteen constants is zero (for details see ZEREN and REYNOLDS (1972)). This characteristic equation determines the neutral state which is obtained when the real part of n is equal to zero. We set $n=0$ to obtain the neutral state. This assumption, that is, exchange of stability, is rather artificial. RICHTER and JOHNSON (1974) found that the real part of n is equal to zero but the imaginary part of n is not, that is, the overstable solution. As their overstable solutions seem to be found in the cases of small density difference, and because of mathematical simplicity, we assume the exchange of stability in this paper. Non-dimensional parameters which control the instability are (1) geometrical factors d_1,* $d_2^*=1-d_1^*$,

that is, the depth of each layer normalized by the total depth, (2) non-dimensional wave number $k^*=kd$ where k is the wave number and d is the total depth of fluids, and (3) differences in the physical properties between two fluids such as the ratio of density, thermal conductivity, etc. We assume that differences exist only in density and viscosity and all the other properties are the same. These assumptions may be suitable for the mantle convection study. In this case, the controlling parameters are the viscosity ratio ν^*, Rayleigh number Ra, dimensionless wave number k^* and RICHTER and JOHNSON's $R\rho$ defined as,

$$\nu^*=\nu_2/\nu_1, \tag{4a}$$

$$Ra=g\alpha_1\beta_1 d^4/(\nu_1\kappa_1), \tag{4b}$$

$$k^*=kd, \tag{4c}$$

$$R\rho=g\Delta\rho d^2/(\rho_1\nu_1\kappa_1), \tag{4d}$$

where β and $\Delta\rho$ are the temperature gradient and density difference between the lower and upper fluids ($\Delta\rho=\rho_2-\rho_1>0$, $\Delta\rho\ll\rho_1$, ρ_2). $R\rho$ is the equivalent Rayleigh number calculated by the density difference $\Delta\rho$ instead of $\rho_1\alpha\Delta T$. We studied three cases,

(A) convection is divided into two equal parts, $d_1^*=d_2^*=1/2$,
(B) convection is divided unequally, $d_1^*=1-d_2^*=1/3$,
(C) the same as (B) but the viscosity ratio (the lower to the upper) is set at 100.

$R\rho$ is set at 10^5 in all the cases. This value is an order of magnitude less than the one suggested by RICHTER and JOHNSON (1974), but there seems to be little difference in the results both in quantity and quality. The eigen Rayleigh number which defines the neutral state is multiple function of wave number k^*. We basically took the lowest eigen Rayleigh number at each k^*. However, when it is found that the corresponding eigen function is not the same type as found before, we adopt such an eigen Rayleigh number, even if it is not the lowest Rayleigh number.

Case (A) is investigated to understand the effects of the insertion of a boundary in the fluid, case (B) is to understand the effect of the non-symmetry in geometry and case (C) is to understand the effects of viscosity differences on the coupling between the upper and lower convections. In the earth, several authors (MCKENZIE and WEISS, 1975; RICHTER, 1979) assume that the convection is divided at a depth of about 700 km, where the deepest earthquakes are observed, corresponding to the ratio d_1^* of about $700/3000\simeq 0.2$. However, because of the sphericity of the real earth and the constraints imposed by the numerical calculations, we choose a d_1^* value of 1/3 tentatively for cases (B) and (C). The viscosity of the earth is one of the most uncertain quantities in the earth science.

Recently, CATHLES (1975) proposed an earth model having an almost uniform viscosity (about 10^{22} poise) and a low viscosity channel under the elastic plate, whereas YOKOKURA (1979) proposed a model consisting of 10^{22} poise in the upper mantle and 10^{24} poise in the lower mantle from the analysis of the dynamic support of the subducting plate. Considering these investigations, we choose the viscosity ratio to be 1 and 100. The calculated neutral stability curves represented in $Ra-k^*$ (i. e., Rayleigh number—wave number) plane are shown in Figs. 2, 4, and 6 for cases (A), (B) and (C) respectively. Now, we will discuss each case briefly.

Case (A)

This is a case having a symmetry. The viscosity of each fluid is the same and the interface is in the middle ($d_1^*=d_2^*=0.5$). The lower curve (1) in Fig. 2 coincides with the usual stability curve of the Rayleigh-Benard convection with stress free top and bottom surfaces and with a depth of $d/2$ as may be easily inferred from the straight intuition (see Appendix 2). Fig. 3a shows the corresponding eigen functions of the

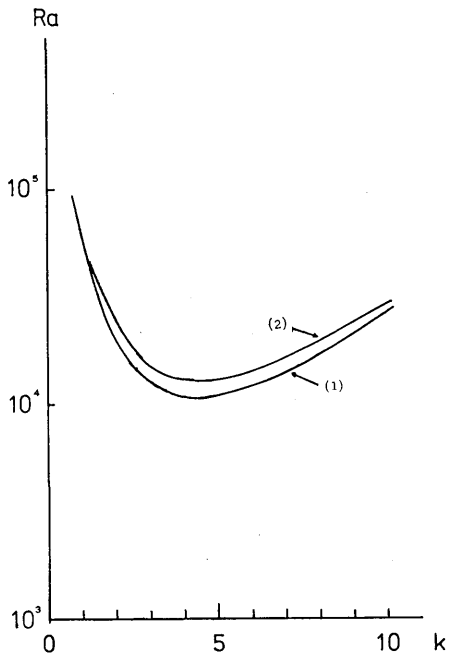

Fig. 2. Marginally stable Rayleigh number as a function of wave number for case (A). R_ρ is set at 10^5 and all the ratios of the other physical properties are set one. Note that the stability curve for the usual Rayleigh-Benard case with a depth of (1/2) d coincides with that for curve (1). Curves (1) and (2) correspond to the 'mechanical coupling' and the 'thermal coupling' respectively.

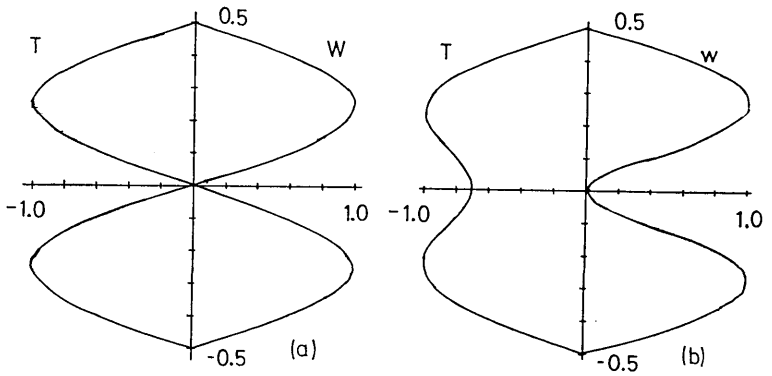

Fig. 3. Eigen functions of velocity and temperature normalized by the maximum value. T means temperature and W vertical component of the velocity. (a) for curve (1) in Fig. 2 ($Ra=1.247\times10^5$, $k^*=2\pi$) and (b) for curve (2) in Fig. 2 ($Ra=1.509\times10^5$, $k^*=2\pi$). As expected, a symmetrical pattern can be observed. Note the differences of the 'mechanical coupling' and the 'thermal coupling'.

vertical component of velocity and temperature in relation to the depth for the representative case. We can see a reversal in the sign at $z=0$ (i.e. the initial interface between two fluids). The upper curve (2) of Fig. 2 is the new state produced by the introduction of the separation in the fluid. Fig. 3b shows the amplitude of the perturbed vertical component of velocity and temperature for the curve (2). There is no change in sign for the velocity at the interface. That means the upper flow goes up where the lower flow goes up. UKAJI and SAWADA (1970a, b, 1971) considered a similar problem and found the same phenomenon and termed the state represented as the curve (1) 'mechanical coupling' and curve (2) 'thermal coupling'. Since this terminology appears appropriate, we will adopt it throughout this paper. According to our results, the main effect of the separation is the emergence of the 'thermal coupling' that will not be observed when the finite amplitude convection is considered as will be shown later in this paper.

Case (B)

In this case the interface is introduced at one third of the total depth ($d_1^*=1-d_2^*=1/3$), and the viscosity of each fluid is the same. It may be inferred that there is a mode which is coincident with the ordinary Rayleigh-Benard convection having two nodes, one of which is the plane of the separation. This mode is curve (2) in Fig. 4 and the perturbed amplitudes of vertical component of velocity and temperature are shown in Fig. 5b. By analogy with case (A), we identify that the curve (3) in Fig. 4 represents the 'thermal coupling' as demonstrated clearly in Fig. 5c. The most unstable mode (curve (1) in Fig. 4), where the lower layer

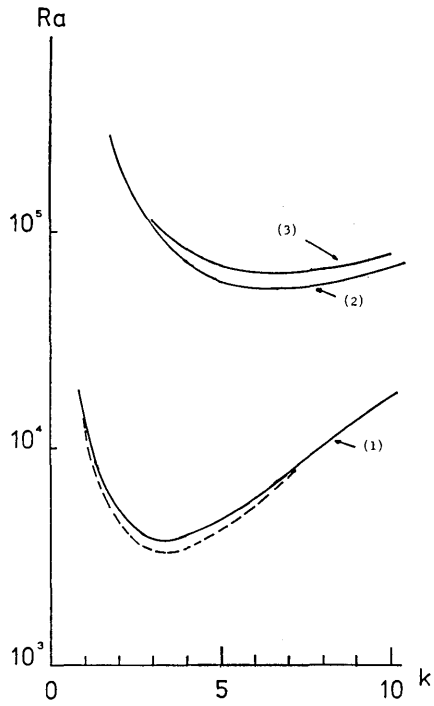

Fig. 4. Marginally stable Rayleigh number as a function of wave number for case (B). The dotted line in the figure shows the usual Rayleigh-Benard stability curves for the lower fluid (see text and Appendix 2). Curve (1) corresponds to the modified 'mechanical coupling' i.e. 'dragging mode' in which the lower layer drags the other. Curves (2) and (3) correspond to the 'mechanical coupling' and the 'thermal coupling' respectively.

is unstable but not the upper layer, is recognized as the mode in which the lower convection 'drags' the upper fluid. This circumstance will be understood from the figure of the velocity and temperature shown in Fig. 5a. This mode is, apparently, a 'mechanical coupling' slightly modified by the non-symmetry between the upper and lower fluids. The dotted line shown in Fig. 4 represents the stability curve of the usual Rayleigh-Benard convection with the depth of $(2/3)d$ and both free surfaces (see Appendix 2). We can recognize that it almost agrees with the most unstable mode. The small difference between them may be explained by saying that since the lower fluid must drag the upper, the interface between them is not completely free, so the situation becomes less unstable.

Case (C)

In this case the interface is at one third of the total depth ($d_1^*=1-d_2^*=1/3$) and the viscosity of the lower fluid is 100 times that of the

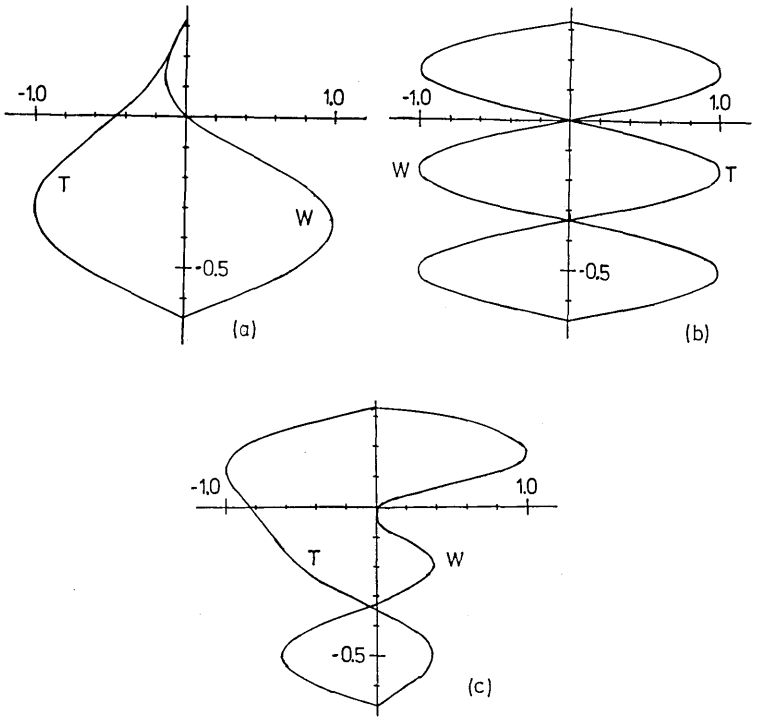

Fig. 5. Eigen functions of velocity and temperature normalized by the maximum value. T means temperature and W vertical component of the velocity. (a) for curve (1) in Fig. 4 ($Ra=3.817\times10^3$ $k^*=\pi$), (b) for curve (2) in Fig. 4 ($Ra=9.741\times10^4$ $k^*=\pi$) and (c) for curve (3) in Fig. 4 ($Ra=1.071\times10^5$ $k^*=\pi$).

upper fluid. There is no exact correspondence of the stability curves with that of the ordinary Rayleigh-Benard convection because of the viscosity difference between the upper and the lower layers. We can expect that there are two modes, i.e. 'dragging mode', in which the upper layer drags the lower, and a mode in which both the upper and the lower layers are unstable. Curve (1) in Fig. 6 is the 'dragging mode' and curve (2) is the latter mode as shown in Figs. 7a and 7b. The dotted lines in Fig. 6 represent the stability curves of the usual Rayleigh-Benard convection with depth of $(1/3)d$, $\nu=\nu_1$ (the lower dotted line) and $(2/3)d$, $\nu=\nu_2$ (the upper dotted line) and both free surfaces. The two modes described before exist between these dotted lines. This is because in the case of curve (1), the upper fluid must drag the lower one and in the case of curve (2) the upper fluid is already moving and the lower one becomes easily unstable compared to the free surface case. There is no 'thermal coupling' mode within the range of our calculations.

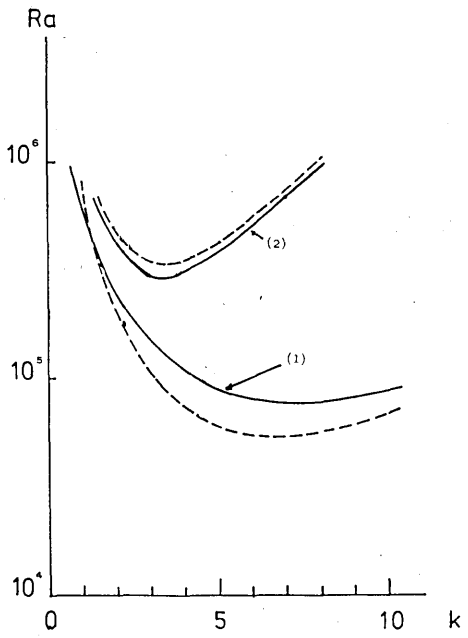

Fig. 6 Marginally stable Rayleigh number as a function of wave number for case (c). Curve (1) is the 'dragging mode' in which the upper layer drags the lower layer because of the combined effect of the non-symmetry in the geometry and differences in the viscosity making the upper layer more unstable than the lower. Curve (2) is the 'mechanical coupling' or 'both unstable mode' in which the lower layer also is unstable. The 'thermal coupling' may disappear at least in the range of our calculations. The dotted lines in the figure show the usual Rayleigh-Benard stability curves for each fluid (see text text and Appendix 2).

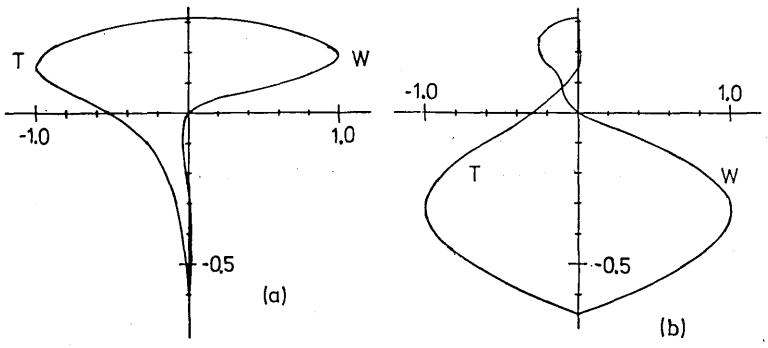

Fig. 7. Eigen functions of velocity and temperature normalized by the maximum value. T means temperature and W vertical component of the velocity. (a) for curve (1) in Fig. 6 ($Ra=7.821\times10^4$, $k^*=2\pi$) and (b) for curve (2) in Fig. 6 ($Ra=5.605\times10^5$, $k^*=2\pi$).

3. Summary of Marginal Stability Analysis

The 'mechanical coupling' and 'thermal coupling' as defined by UKAJI and SAWADA (1970a, b, 1971) were found to exist. However, it seems that the 'thermal coupling' may emerge only when the layered convection system satisfies some specific conditions, because the 'thermal coupling' does not appear in case (C). Also, the 'thermal coupling' is the more excited state than the 'mechanical coupling'. Probably a more interesting point that we discovered in the marginal stability analysis is the fact that some of the neutral stability curves can be approximately explained by those of each fluid. Similar result will be found later when we consider the case in which the amplitude of convection becomes finite.

4. An Analysis with Finite Amplitude Convection

In the treatment of the finite amplitude convection, we make the following assumptions in addition to those described in the previous section.

(1) The convection is a roll type, i.e. two-dimensional convection is assumed.
(2) The interface between the lower and the upper layers is fixed.
(3) The Prandtl number is infinite.

The assumption (1) will be, for a certain range of the Rayleigh number, incorrect because both experiments and theories show three-dimensional nature of the flow regime (BUSSE, 1967; BUSSE and WHITEHEAD, 1971). However, if the flow in the mantle is two-scaled as suggested by RICHTER (1973) and RICHTER and PARSONS (1975), the assumption of the roll type convection may be valid for the small scale convection. In their two-scaled convection, one is the large scale flow accompanied by the movement of plate and the other is the roll type small scale flow produced by the secondary instability and aligned with the direction of the shear flow induced by the plate motions. We also think that the general nature of the convection such as the efficiency of the heat transport will be well described by the analysis of the two-dimensional convection (for example, compare the results of MOORE and WEISS, (1973) with those of ROSSBY (1969)). The assumption (2) is uncertain because this assumption leads to discontinuity of pressure and must be checked by further empirical and/or theoretical investigations. If the lower fluid is much heavier than the upper fluid, this assumption may be valid. The assumption (3) seems to be well established because the Prandtl number for the mantle is about $10^{24} \gg 1$ implying that the

Reynolds number is small and the intertia term can be neglected in comparison with the buoyancy and viscous terms. Following the non-dimensional scheme of RICHTER (1973), that is,

$$\boldsymbol{r}=d\boldsymbol{r}^*, \tag{5a}$$

$$\boldsymbol{u}=\frac{\kappa}{d}\boldsymbol{u}^*, \tag{5b}$$

$$T=\Delta T\, T^*, \tag{5c}$$

$$t=\frac{d^2}{\kappa}t^*, \tag{5d}$$

where asterisks denote the dimensionless values, and applying these schemes to equation (2), we obtain the basic non-dimensional equations describing the layered convection as follows;

$$\nabla^2\omega_i^*=Ra\frac{1}{\gamma_i}\frac{\partial T_i^*}{\partial x^*} \qquad \text{where} \qquad \left(\gamma_1^*=1,\ \gamma_2^*=\frac{\nu_2}{\nu_1}\right), \tag{6a}$$

$$\nabla^2\psi_i^*=\omega_i^*, \tag{6b}$$

$$\frac{DT^*}{Dt^*}=\nabla^2 T_i^*, \tag{6c}$$

where ψ_i^* is the stream function, ω^* is the y-component of the vorticity and Ra is the Rayleigh number that are defined respectively as,

$$\boldsymbol{u}_i^*=\left(\frac{\partial\psi_i^*}{\partial z^*},\ -\frac{\partial\psi_i^*}{\partial x^*}\right), \tag{7a}$$

$$\omega_i^*=(\boldsymbol{rot}\ \boldsymbol{u}_i^*)_y=\nabla^2\psi_i^*, \tag{7b}$$

$$Ra=\frac{g\alpha_1 d^3\Delta T}{\nu_1\kappa_1}, \tag{7c}$$

where $\Delta T=T$(bottom surface)$-T$(top surface). The boundary conditions, are,

$\psi_1^*=0$	(zero vertical velocity)	(8a)	at $z^*=d_1^*$,
$\omega_1^*=0$	(zero shear stress)	(8b)	
$\psi_2^*=0$	(zero vertical velocity)	(8c)	at $z^*=-d_2^*$,
$\omega_2^*=0$	(zero shear stress)	(8d)	
$\frac{\partial\psi_1^*}{\partial z^*}=\frac{\partial\psi_2^*}{\partial z^*}$	(continuity of horizontal velocity)	(8e)	at $z^*=0$.
$\psi_1^*=\psi_2^*=0$	(fixed interface and the continuity of vertical velocity)		
$\frac{\partial T_1^*}{\partial z^*}=\frac{\partial T_2^*}{\partial z^*}$	(continuity of heat flux)	(8f)	
$T_1^*=T_2^*$	(continuity of temperature)	(8g)	

In solving these equations, we adopted essentially the same finite difference method as RICHTER (1973) except for the integrating techniques of Poisson's equations by SOR (Successive Over Relaxation method, see, for example, ROACHE, 1978) which is simpler in programming. The boundary conditions at the upper and the lower surfaces are easily fulfilled by applying the conditions $\psi^*=$constant and $\omega^*=0$ at the surface. Also, the conditions concerning the conservation of energy and the continuity of temperature at the interface are easily satisfied. The problem is the combined conditions of the continuity of the horizontal component of velocity and tangential stress at the interface that requires the appropriate choice of ω^* at the interface in order not to violate the continuity of velocity at $z^*=0$, i.e. $u_1^*=u_2^*$. These situations are also encountered when the synthesized flow field of the plate moving at a constant speed and the thermal convection are investigated (RICHTER, 1973; LUX *et al.*, 1978). This is based on the physical fact that the tangential stress is derived from the vertical gradient of the horizontal component of the velocity. To avoid these difficulties, we adopt the modified iterative scheme proposed by RICHTER (1973). The $(k+1)$-th ω^* at the boundary between the two fluids is derived from the k-th flow field according to the equation,

$$\omega^{*(k+1)}_{boundary}=\omega^{*(k)}_{boundary}+\delta(u^{*(k)}_{boundary,L}-u^{*(k)}_{boundary,U}), \tag{9}$$

where the subscript 'boundary' denotes the value at the interface between the lower and the upper fluids, δ is an appropriate constant which must be determined by trial and error, and L implies the value deduced from the lower layer and U from the upper layer. Iteration is repeated until a satisfactory convergence of ω^* is obtained. The condition of the continuity of the vertical component $w_1^*=w_2^*=0$ (that is, the interface is fixed) can be expressed as $\psi^*=$constant at $z=0$. This rather artificial condition of $w_1^*=w_2^*=0$ gives no assurance of the continuity of the normal stress at the boundary. In this regard we call our calculation a 'pseudo' layered convection. Other boundary conditions are the conditions at the sides because the calculation must be executed within a finite space. The symmetric boundary conditions in temperature (i.e., no heat is transmitted through the side boundaries) and the anti-symmetric conditions in the velocity field (i.e. zero shear stress is assuemd) were adopted. The aspect ratio of the box, in which numerical integrations were made, of the vertical to the horizontal (strictly speaking, the wave length of the convection) is important because of its influence on the efficiency of heat transport (see MOORE and WEISS, 1973). However, for various reasons (e.g. computer time or money), it was restricted to 1:1, when we considered the usual Rayleigh-Benard case and case (A) described

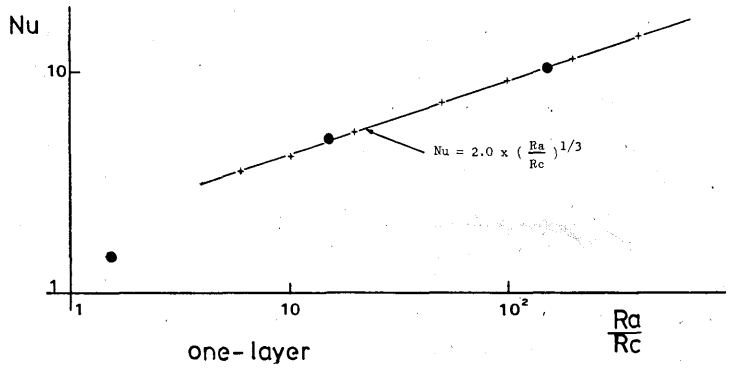

Fig. 8. Relations between the Nusseldt number (Nu) and the Rayleigh number (Ra) in the usual Rayleigh-Benard case. Crosses in the figure are the values obtained numerically by MOORE and WEISS (1973). Solid circles show the values obtained in the present study. The line shows $Nu=2.0\times(Ra/Rc)^{1/3}$ which can approximately explain MOORE and WEISS' results. Rc is the minimum critical Rayleigh number of 657.5 for both free surfaces (CHANDRASEKHAR, 1961).

in the preceding section, and to 1:2 for cases (B) and (C). The mesh design is also important in the calculations. For the same reasons as above, however, it was selected to be 11×11 or 21×21 for the case of aspect ratio of one, and 16×31 for the other cases. The calculation was started by adding an initial perturbation, which was either sinusoidal temperature perturbation or a flow field previously obtained for a different Rayleigh number. The calculation was continued until the steady or sufficiently stable state was obtained. To check the accuracy of this method, we calculated the Nusseldt number of the usual Rayleigh-Benard convection having the aspect ratio of one and compared the results with those of MOORE and WEISS (1973) (Fig. 8). The Nusseldt number is calculated at the depth near the middle of the convecting fluid as was done by MOORE and WEISS (1973) according to the following equation

$$Nu=\overline{w^*T^*-\frac{\partial T^*}{\partial z^*}}, \tag{10}$$

where the upper bar means the horizontal average of quantities. The results obtained well coincide with those of MOORE and WEISS (1973), which is approximately expressed as $Nu\simeq2.0\times(Ra/Rc)^{1/3}$ where Rc is the minimum critical Rayleigh number of $657.5=27\pi^4/4$ (see Fig. 8). In the following calculations, we figured out the Nusseldt number near the middle of each layers according to the equation (10). The effect of the aspect ratio of the box used in the numerical calculation on the convection is not fully studied in this paper. Although MOORE and WEISS (1973)

reported that a maximum of about 20% difference in the Nusseldt number exists when the aspect ratio was changed with the same Rayleigh number, we believe that the general nature of the heat transport shown in this paper does not change substantially.

The calculations for the layered case were checked by comparing the velocity amplitude obtained by the finite difference method in the range of small departure from the critical Rayleigh number, i.e. $Ra/Rc \simeq 1$, with those calculated by the marginal stability analysis. Fairly agreeable results were obtained in cases (A) and (B). Slight discrepancies were found in case (C) in the lower layer. However, because the amplitude in the lower layer is much smaller than in the upper, we do not consider these discrepancies critical.

Case (A)

In this case, the interface is in the middle ($d_1^* = d_2^* = 0.5$) and the viscosity of each layer is the same. The calculated Nusseldt number in relation to the normalized Rayleigh number Ra/Rc and the flow field, that is, the stream lines, the vorticity and the temperature of typical cases are shown in Fig. 9 and Fig. 10. The definition of Rayleigh number is the same as the equation (4 b) described in the preceding section, that is, the Rayleigh number defined by assuming that the fluid of the upper layer extends throughout the whole layer. The same definition of the Rayleigh number will be used in the following analysis. Rc is the minimum critical Rayleigh number of 657.5 for the usual Rayleigh-Benard case. In Fig. 9, the obtained Nusseldt number is shown by the black dots and also the $Nu-Ra$ relation of usual Rayleigh-Benard convection

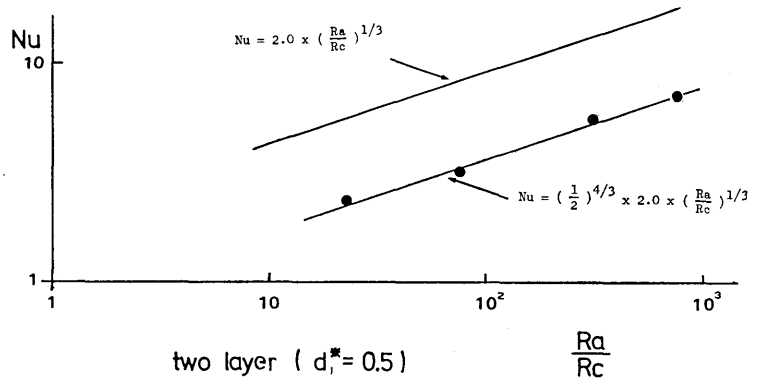

Fig. 9. Nu-Ra relation obtained for case (A). Rc is the minimum critical Rayleigh number for ordinary case, 657.5. Calculated Nusseldt numbers are shown by solid circles. Solid lines are Nu-Ra relation for the usual Rayleigh-Benard convection ($Nu = 2 \times (Ra/Rc)^{1/3}$) and the curve obtained by the simple parameterization for the layered convection (see Section 5).

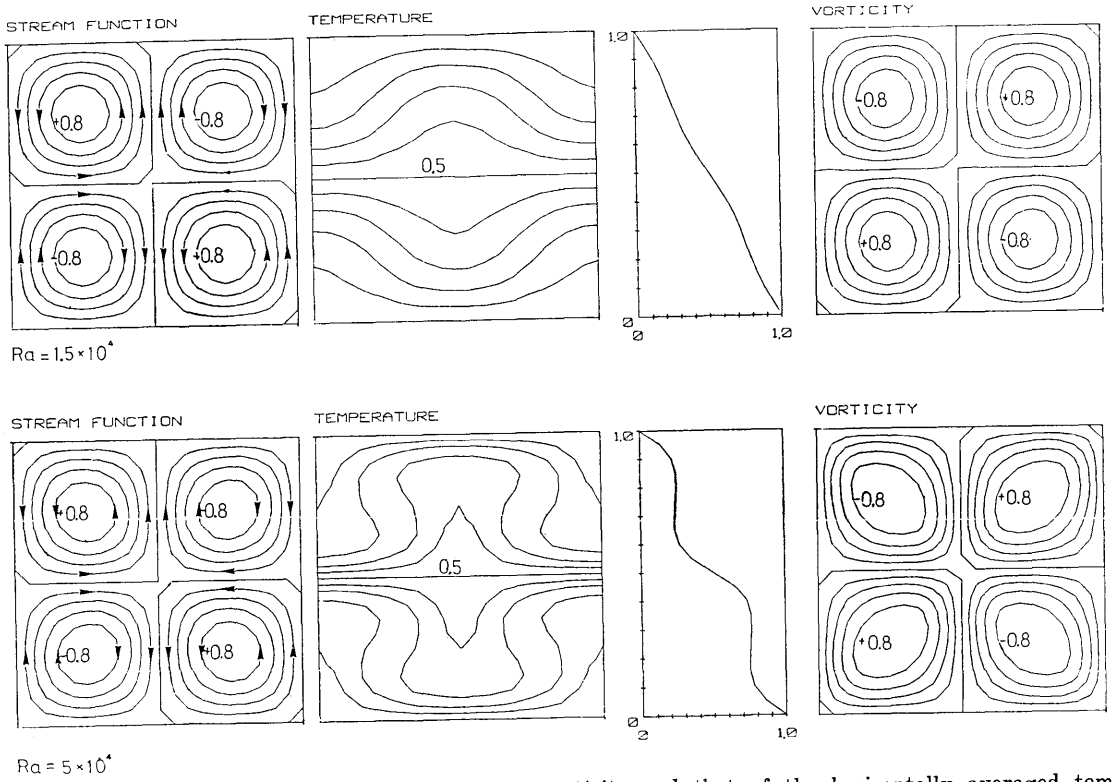

Fig. 10 a. Distribution of stream function, temperature, vorticity and that of the horizontally averaged temperature with relation to the depth for case (A) with $Ra=1.5\times10^4$. Contours show iso-value lines. All values are normalized by maximum absolute value, that is $|\phi|\max=1.77$ and $\omega\max=1.38$. A highly symmetrical pattern of convection is observed.

Fig. 10 b. Same as 10 a for case (B) with $Ra=5\times10^4$. Values used for the normalization are $|\phi|\max=8.26$ and $|\omega|\max=584$. Thermal boundary layers appear both in the upper and lower layers. Note that in both Figs. 10 a and 10 b the temperature and vorticity are almost 0.5 and 0 at the interface between the two immiscible fluids.

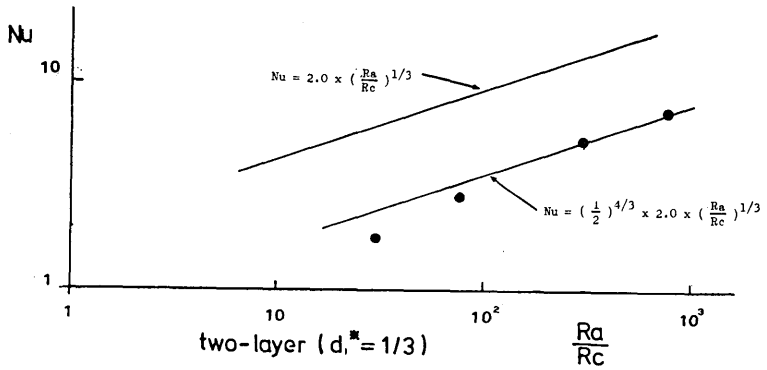

Fig. 11 *Nu-Ra* relation obtained for case (B). *Rc* is the minimum critical Rayleigh number of 657.5 (see figure caption of Fig. 9 for detail).

($Nu=2\times(Ra/Rc)^{1/3}$) is included. The other line shown in Fig. 9 is obtained by the simple parameterization for a two-layer convection that will be described in a later section. In the following figures of the $Nu-Ra$, the same style will be adopted. From this figure, we can find that the layered convection is less effective in transporting the heat than the one-layer convection. This is because the large scale motion is inhibited by the interface and there is a conductive layer near the interface. As seen in Figs. 10a and 10b a highly symmetrical pattern of convection appears as might be expected. Well developed thermal boundary layers are formed at the top, at the bottom and at the interface when Ra becomes large compared to the critical Rayleigh number as in the case of the ordinary Rayleigh Benard convection (see Fig. 10b). The flow pattern is of the 'mechanical coupling' mode. However, it may be noted that the shear stress at the interface, being easily derived from the value of the vorticity, is nearly zero. This means that the coupling is achieved almost in the shear stress free state. Note also that the temperature at the interface is 0.5 as can be expected from the symmetry.

Case (B)

In this case situation different from case (A) occur, because the interface is at one third of the total depth ($d_1^*=1-d_2^*=1/3$) with constant viscosity throughout the whole layer. However, the calculated Nusseldt number shown in Fig. 11 shows that the $Nu-Ra$ relation is nearly the same as that in case (A) in spite of the difference in geometry. This result can be simply explained by the parameterized analysis as will be described in section 5. The flow field, stream lines and temperature in this case are non-symmetric (see Fig 12). If Ra lies between the states of the 'dragging mode' and the 'mechanical couping' mode, the lower

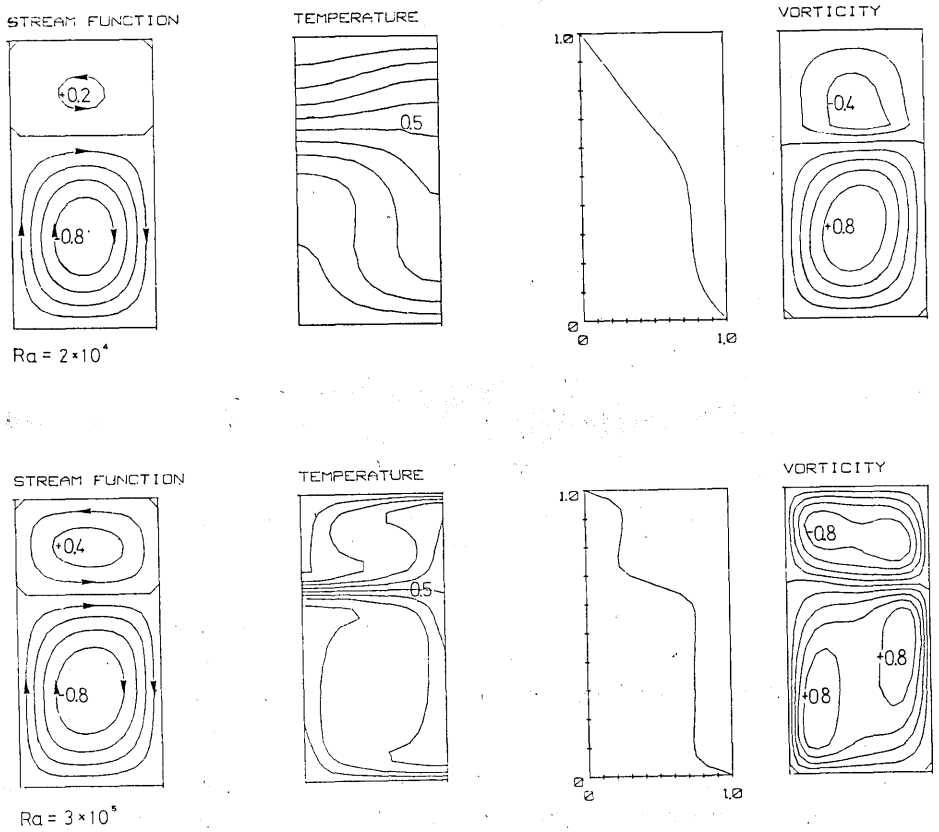

Fig. 12a Distributions of stream function, temperature, vorticity and that of the horizontally averaged temperature with relation to the depth for case (B) with $Ra=2\times10^4$. Contours show the iso-value lines. All values are normalized by the maximum absolute value, that is $|\psi|\max=4.31$ and $|\omega|\max=264$. Thermal boundary layers are formed in the lower part of the fluid in contrast to the upper implying that the lower fluid drags the upper.

Fig. 12b. Same as Fig. 12a for case (B) with $Ra=3\times10^5$. Values used for the normalization are $|\psi|\max=34.3$ and $|\omega|\max=1990$. Both in the lower and the upper fluids well developed thermal boundary layers are formed. Note that at the interface between the two fluids the temperature and vorticity are almost 0.5 and 0 respectively.

fluid, being more unstable than the upper, evidently drags the upper fluid as observed in the figure of the vorticity, that is, the zero vorticity line is in the lower layer and the vorticity is negative along the interface (Fig. 12a). The thermal boundary layer in the lower layer develops more rapidly than in the upper as Ra becomes greater. Finally, with a high Ra the boundary layers appear in both the upper and the lower fluids (see Figs. 12a and 12b). Although many features of the flow field

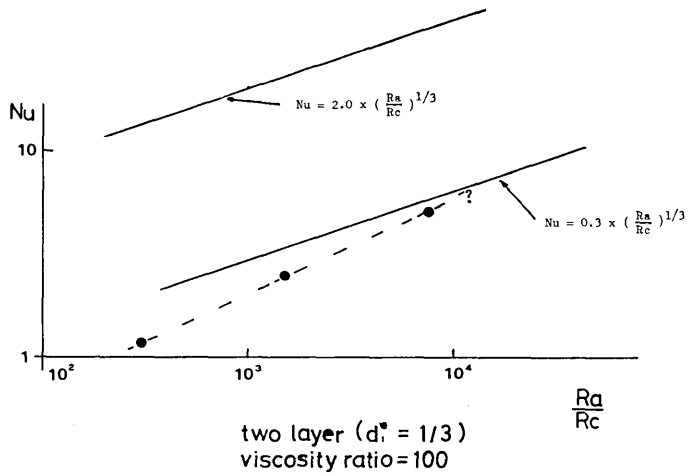

Fig. 13. *Nu-Ra* relations obtained for case (C). *Rc* is the minimum critical Rayleigh number of 657.5. (See figure caption of Fig. 9 for details.)

are different from case (A), it must be noted that the horizontally averaged temperature and shear stress acting on the interface are nearly 0.5 and 0 respectively, when the Rayleigh number becomes large.

Case (c)

In this case, the viscosity of the lower fluid is 100 times greater than that of the upper, and the interface is at one third of the total depth. The calculated Nusseldt number versus the normalized Rayleigh number is shown in Fig. 13. Like the other cases, there is a clear degradation in the ability of transporting the heat. In Fig. 14a, we show the 'dragging mode' in which only the upper layer is unstable. When the Rayleigh number is small, the double cell appear in the lower part of the fluid that agrees qualitatively with the marginal stability analysis (see Figs. 7a and 14a). While, in Fig. 14a, vague boundary layers develop in the upper layer, well developed boundary layers appear both at the top, at the bottom, and at the interface in the case of Fig. 14b where both layers are unstable. The interface temperature is about 0.2 to 0.3 and the zero vorticity line is in the upper fluid, suggesting that the upper layer is slightly dragging the lower layer. (Note that in the lower layer we show the vorticity multiplied by the viscosity ratio of 100). The lower temperature at the interface compared to cases (A) and (B) will be explained by the effect of the difference in the viscosity in the next section.

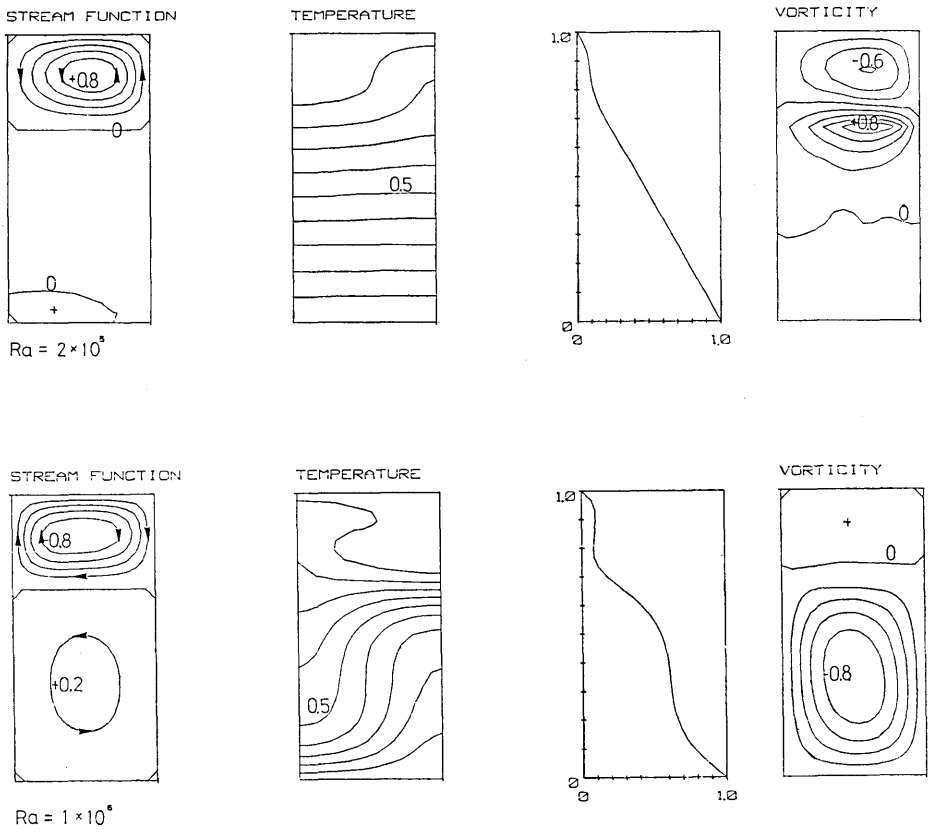

Fig. 14a Distribution of stream function, temperature, vorticity (here in the lower fluid we show the vorticity multiplied by the viscosity ratio of 100) and the horizontally averaged temperature with relation to the depth for case (C) with $Ra=2\times10^5$. Contours show the iso-value lines. All values are normalized by the maximum absolute values, that is, $|\psi|\max=3.76$ and $|\omega|\max=993$. Thermal boundary layers are formed in the upper part of the fluid in contrast to the lower, implying that the upper fluid drags the lower.

Fig. 14b. Same as Fig. 14a for case (C) with $Ra=1\times10^6$. The values used for the normalization are $|\psi|\max=35.6$ and $|\omega|\max=6.97\times10^4$. Both in the lower and the upper fluids well developed thermal boundary layers are formed. Note that at the interface between two fluids the temperature is almost in the range of 0.2 to 0.3 and the zero vorticity line slightly penetrates into the upper fluids.

5. Application of Simple Parameterization

In the ordinary Rayleigh-Benard convection system, the relation between the Nusseldt number and the Rayleigh number is roughly expressed as,

$$Nu=b\left(\frac{Ra}{Rc_0}\right)^a, \tag{1}$$

where a and b are constants of about 0.3 and 1. Rc_0 is the minimum critical Rayleigh number of 657.5. MOORE and WEISS (1973) showed that $a=1/3$ and $b=2.0$ in the case of the infinite Prandtl number with both free surfaces. This is also confirmed by our study (see Fig. 8). If we assume that the above relation is valid independently in both the upper and the lower convecting fluids, the continuity of heat flow at the interface requires the following equation (HONDA, 1980)

$$b\left(\frac{Ra_1}{Rc_0}\right)^a \times k_1 \frac{\Delta T_1}{d_1} = b\left(\frac{Ra_2}{Rc_0}\right)^a \times k_2 \frac{\Delta T_2}{d_2}, \tag{11}$$

where Ra_i and ΔT_i are the locally defined Rayleigh number and the temperature difference as follows,

$$Ra_i = \frac{g\alpha_i \Delta T_i d_i^3}{\nu_i \kappa_i}, \tag{12a}$$

$$\Delta T_1 = T(\text{at the interface}) - T(\text{at the top surface}), \tag{12b}$$

$$\Delta T_2 = T(\text{at the bottom surface}) - T(\text{at the interface}). \tag{12c}$$

We denote the total temperature difference between the top and bottom surfaces as ΔT. Then,

$$\Delta T = \Delta T_1 + \Delta T_2, \tag{12d}$$

From the equations (11) and (12d), we obtain,

$$\Delta T_1 = \frac{\alpha'}{1+\alpha'} \Delta T, \tag{13a}$$

$$\Delta T_2 = \frac{1}{1+\alpha'} \Delta T, \tag{13b}$$

where

$$\alpha' = \left(\frac{\nu_1}{\nu_2}\right)^{\frac{a}{1+a}} \left(\frac{d_2}{d_1}\right)^{\frac{3a-1}{1+a}} \tag{13c}$$

(Note that $\alpha_1=\alpha_2$, $\kappa_1=\kappa_2$). Changing the locally defined Rayleigh number Ra_i into the ordinary Rayleigh number Ra ($Ra=g\alpha_1 \Delta T d^3/(\nu_1\kappa_1)$), we obtain the heat flux carried by the convection Q as,

$$Q = b\left(\frac{Ra_1}{Rc_0}\right)^a k_1 \frac{\Delta T_1}{d_1} = b\left(\frac{Ra_2}{Rc_0}\right)^a k_2 \frac{\Delta T_2}{d_2}$$

$$=b\left(\frac{\alpha'}{1+\alpha'}\right)^{a+1}\left(\frac{d_1}{d}\right)^{3a-1}\left(\frac{Ra}{Rc_0}\right)^{a}k_1\frac{\Delta T}{d}. \tag{14}$$

Thus, the 'theoretical' $Nu-Ra$ relation becomes,

$$Nu=\frac{Qd}{k_1\Delta T}=b\left(\frac{\alpha'}{1+\alpha'}\right)^{a+1}\left(\frac{d_1}{d}\right)^{3a-1}\left(\frac{Ra}{Rc_0}\right)^{a}. \tag{15}$$

This equation says that, although the magnitude of Nu is varied, the slope obtained from the semi-log plot of Ra and Nu does not change as observed in Figs. 9 (case (A)), and 11 (case (B)), although in case (C) this relation does not hold well as seen in Fig. 13. To check the magnitude of Nu, we give the values of $a=1/3$ and $b=2$, and get

$$\Delta T_1=\frac{(\nu_1/\nu_2)^{1/4}}{1+(\nu_1/\nu_2)^{1/4}}\Delta T, \tag{16a}$$

$$\Delta T_2=\frac{1}{1+(\nu_1/\nu_2)^{1/4}}\Delta T, \tag{16b}$$

$$Nu=2\left(\frac{(\nu_1/\nu_2)^{1/4}}{1+(\nu_1/\nu_2)^{1/4}}\right)^{4/3}\left(\frac{Ra}{Rc_0}\right)^{1/3}. \tag{16c}$$

This result is rather surprising, because the temperature at the interface and the Nusseldt number do not apparently depend on geometry. This fact is already shown for cases (A) and (B). If we consider cases (A) and (B), i.e. $\nu_1/\nu_2=1$, then we get,

$$\Delta T_1=\Delta T_2=0.5\Delta T, \tag{17a}$$

$$Nu=2\left(\frac{1}{2}\right)^{4/3}\left(\frac{Ra}{Rc_0}\right)^{1/3}=0.79\left(\frac{Ra}{Rc_0}\right)^{1/3}. \tag{17b}$$

The equation (17b) is shown in Figs. 9 (case (A)) and 11 (case (B)). These figures show that the agreement between the finite amplitude calculation and parametrized theory is good. For case (C) i.e. $\nu_2/\nu_1=100$, we get,

$$\Delta T_1=0.24\Delta T, \tag{18a}$$

$$\Delta T_2=0.76\Delta T, \tag{18b}$$

$$Nu=0.30\left(\frac{Ra}{Rc_0}\right)^{1/3}. \tag{18c}$$

As mentioned before, the mean temperature at the interface for case (C) is in the range of about 0.2 to 0.3. This agrees fairly well with the value of 0.24 obtained by simple parameterization. In Fig. 13, equation (18c) is shown. The Nusseldt numbers calculated by the finite amplitude calculation are found to be close to those predicted by the equation (18c).

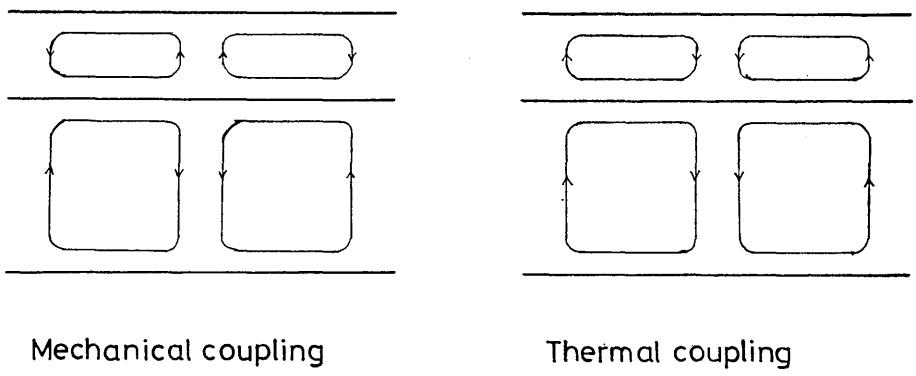

Fig. 15. Schematic view of the 'mechanical coupling' and the 'thermal coupling'. Also see UKAJI and SAWADA (1970a, b, 1971).

The small disciscrepancy may be caused by the strong mechanical coupling between the upper and the lower layers. However, further study is required because the calculations have been made only in a limited range of Ra and the accuracy of the calculation is not very high.

6. Conclusions and Discussions

The marginal stability and finite amplitude analysis of the convection in which two immiscible fluids are initially stratified and heated from below are presented.

In the marginal stability analysis, we find two types of coupling between the two fluids as previously pointed out by UKAJI and SAWADA (1970a, b, 1971). One is the 'mechanical coupling' in which flows near the interface have the same horizontal direction, that is, the upper convecting fluid goes up where the lower one goes down. The other type is the 'thermal coupling' in which the fluids flow in an opposite horizontal direction near the interface, that is, the upper convecting fluid goes up where the lower one goes up. These two types of convection are schematically shown in Fig. 15. If one of the two fluids is more unstable, there appears a modified mode of the 'mechanical coupling'. Tentatively we name this the 'dragging mode', because the more unstable layer drags the less unstable layer. The 'thermal coupling' mode will probably be the more excited state than the 'mechanical coupling' mode as deduced from the stability curves and appears when the upper and the lower fluids satisfy some specific conditions. In all the cases in which the 'thermal coupling' appears, the difference in the properties of the upper and lower fluids is very small. We may need further studies on the 'thermal coupling'.

Another important result revealed by the marginal stability analysis is the simple explanation of the stability curves. That is, the neutral stability curves for layered convections are well described by the stability analysis of the individual layers with free boundaries at least for the case of 'mechanical coupling' mode.

Next, we calculated the finite amplitude convection of the 'pseudo' layered convection. Only the 'mechanical coupling' is observed. Fairly complex patterns are observed in temperature, stream lines and vorticity. Well developed thermal boundary layers are formed at the upper and lower boundaries and at the interface, when the Rayleigh number becomes many times greater than the critical Rayleigh number. The appearance of the boundary layers can be easily inferred from the usual Rayleigh-Benard case. The $Nu - Ra$ relations for the layered convection can be interpreted by the simple linear combinations of two independently convecting fluids. This is probably because the shear stress free condition and the constant temperature condition are almost satisfied at the interface. In the case of a great difference in the viscosity, in which the shear stress free surface lies in the less viscous fluid (more unstable layer), there may be a possibility of the breakdown of the simple parameterization because of the strong coupling. We also investigated a case in which the interface is assumed to be shear stress free. Preliminary results show the appearence of the 'thermal coupling' mode. This may be inferrable, because the 'mechanical coupling' is suppressed. The interesting point is that the Nusseldt number for this case seems to be larger than that of the 'mechanical coupling'. A possible explanation for this is given below. In the 'mechanical coupling', the cold plume from the top surface is heated up at the interface by the hot plume coming from the bottom surface so that fairly uniform temperature will appear at the interface. However, in the 'thermal coupling' the cold plume from the top surface will sink down where the cold plume forming at the interface sinks down. On the contrary, the hot plume from the bottom surface will go up where the hot plume forming at the interface goes up. As a result, the temperature in the fluids will be more vigourously mixed than in the 'mechanical coupling'. This implies that the 'thermal coupling' can transport heat more effectively than the 'mechanical coupling'. In the mantle, the cause of the separation of the convection and even the existence of the layered convection are not clear so that the nature of the interface is also unknown. If the low viscosity zone exists between the two convections, the 'thermal coupling' may occur. The existence of the low viscosity zone, for example, is suggested by Sammis (1976) who stressed the importance of the transformational super plasticity which may occur in the polymorphic phase boundaries.

Recently, RICHTER and MCKENZIIE (1981) studied a similar problem by both theory and experiments. Their studies are mostly restricted to the symmetrical case with the viscosity ratio of one (case (A)). They showed by experiment that the mixing of whole layers occurs when the density difference between two fluids are almost the same as that caused by the temperature difference. Also their experiments revealed that the coupling of the convections is more complex than that we have studied. This complexity may occur because of the deformation of the interface which we could not model.

The dominant wave length of the convection is not clear, although a numerical experiment with the aspect ratio (horizontal to vertical) of 1 : 2 for case (B) showed that the convection having three cells, which may be the dominant mode of the lower (more unstable) layer, appeared in spite of the one cell initial perturbation. These results may have possible importance in considering the relation between the plate tectonics and convection. Application of the present results on mantle convection problems will be made in another paper.

7. Aknowledgment

I am grateful to Drs. Seiya UYEDA (Earthquake Research Institute, University of Tokyo) and Masanori SAITO (Geophysical Institute, University of Tokyo) who read the manuscript critically and made many suggestions. I also thank Dr. Kinjiro KAJIURA of the Earthquake Research Institute, University of Tokyo for his review of the manuscript. Computations were done by using the computer resources of the Earthquake Prediction Data Center of the Earthquake Research Institute, University of Tokyo.

Appendix 1

List of symbols

d: total depth of convecting layer $d=d_1+d_2$
d_1: depth of the upper fluid
d_2: depth of the lower fluid
g or $\boldsymbol{g}$: gravity or gravity vector
k: thermal conductivity or wave number
Nu: Nusseldt number
p: pressure
$\boldsymbol{r}$: position vector
Ra: Rayleigh number
R_ρ: see text for definition

Rc, Rc_0: minimum critical Rayleigh number for the usual Rayleigh-Benard case
t: time
T: temperature
ΔT: temperature difference between the top and bottom surfaces
$\boldsymbol{u}$: velocity vector
u: horizontal component (x) of the velocity
v: horizontal component (y) of the velocity
w: vertical component (z) of the velocity
x: one of the axis lying in the horizontal plane
y: one of the axis lying in the horizontal plane
z: vertical axis, positive upward
α: coefficient of the volume thermal expansion
β: temperature gradient when the instability does not begin
η: dynamic viscosity
θ: perturbed temperature
κ: thermal diffusivity
ν: kinematic viscosity
ν^*: viscosity ratio
ρ: density
$\Delta\rho$: density difference defined by $(\rho_2-\rho_1)$
ϕ: stream function
ω: y component of vorticity

Appendix 2

Inferrence of the minimum Rayleigh numberr required to generate an instability

The stability curve in the wave number-Rayleigh number space for the usual Rayleigh-Benard convection having both free surfaces is expressed as

$$Rc=\frac{(k'^2+n^2\pi^2)^3}{k'^2} \qquad (2.1),$$

where k' and n are the normalized wave number by the depth of convection and degrees of the eigen function having $(n-1)$ nodal planes in the fluid (CHANDRASEKHAR, 1961). The 'local' Rayleigh number in each fluid can be defined as,

$$Ra_i=\frac{g\alpha_i\beta_i d_i^4}{\nu_i\kappa_i} \qquad (i=1,\ 2) \qquad (2.2).$$

If the upper layer is more unstable than the lower, marginal state may be derived from

$$Ra_1 = Rc. \tag{2.3}$$

Modifying this equation by the use of our definition of Ra and considering the definition of non dimensional wave number, we obtain the critical Rayleigh number Ra as,

$$Ra = Ra_1\left(\frac{d}{d_1}\right)^4 = Rc\left(\frac{d}{d_1}\right)^4 = \frac{\left\{\left(k^*\frac{d_1}{d}\right)^2 + n^2\pi^2\right\}^3}{\left(k^*\frac{d_1}{d}\right)^2}\left(\frac{d_1}{d}\right)^4. \tag{2.4}$$

The least stable degree is the case of $n=1$, then,

$$Ra = \frac{\left\{\left(k^*\frac{d_1}{d}\right)^2 + \pi^2\right\}^3}{\left(k^*\frac{d_1}{d}\right)^2}. \tag{2.5}$$

The minimum value of Ra is obtained when $k^*d_1/d = \pi/\sqrt{2}$, that is,

$$Ra_{min} = 657.5\left(\frac{d}{d_1}\right)^4. \tag{2.6}$$

Essentially the same procedure can be executed, if the lower fluid is more unstable. Results are,

$$Ra = \frac{\left\{\left(k^*\frac{d_2}{d}\right)^2 + \pi^2\right\}^3}{\left(k^*\frac{d_2}{d}\right)^2}\left(\frac{d_2}{d}\right)^4\frac{\nu_2}{\nu_1}, \tag{2.7a}$$

$$Ra_{min} = 657.5\left(\frac{d}{d_2}\right)^4\frac{\nu_2}{\nu_1} \quad \text{at} \quad k^* = \frac{\pi}{\sqrt{2}}\frac{d}{d_2}. \tag{2.7b}$$

References

ANDERSON, D. L., 1980, Early evolution of the mantle, *Episodes*, **1980**, 3-7.

BUSSE, F. H., 1967, On the stability of two dimensional convection in a layer heated from below, *J. Math. Phys.*, **46**, 140-150.

BUSSE, F. H., and J. A. WHITEHEAD, 1971, Instabilities of convection rolls in a high Prandtl number fluid, *J. Fluid Mech.*, **47**, 305-320.

CATHLES, L. M., 1975, Viscosity of the earth's mantle, Princeton University Press, New Jersy, pp. 386.

CHANDRASEKHAR, S., 1961, Hydrodynamic and Hydromagnetic stability, Claredon Press, Oxford, pp. 652.

DAVIES, G. F., 1977, Whole mantle convection and plate tectonics, *Geophys. J. R. astr. Soc.*, **49**, 459-486.

ELSASSER, W. M., P. OLSON and B. D. MARSH, 1979, The depth of mantle convection, *J. Geophys. Res.*, **84**, 147-155.

HONDA, S., 1980, On the layered convection, *Programme and Abstracts*, The Seismological Society of Japan, **1**, 58. (in Japanese)

JARVIS, G. T., and D. P. MCKENZIE, 1980, Convection in a compressible fluid with infinite Prandtl number, *J. Fluid Mech.*, **96**, 515-583.

LUX, R. A., G. F. DAVIES and T. H. THOMAS, 1979, Moving lithospheric plates and mantle convection, *Geophys. J. R. astr. Soc.*, **57**, 209-228.

MCKENZIE, D. P., J. M. ROBERTS and N. O. WEISS, 1974, Convection in the earth's mantle; Towards a numerical simulation, *J. Fluid Mech.*, **62**, 465-538.

MCKENZIE, D. P., and N. O. WEISS, 1975, Speculations on the thermal and tectonic history of the earth, *Geophys. J. R. astr. Soc.*, **42**, 131-174.

MOORE, D. R., and N. O. WEISS, 1973, Two-dimensional Rayleigh-Benard convection, *J. Fluid Mech.*, **58**, 289-312.

RICHTER, F. M., 1973, Dynamical models for sea floor spreading, *Rev. Geophys. Space Phys.* **11**, 223-287.

RICHTER, F. M., 1979, Focal mechanisms and seismic energy release of deep and intermediate earthquakes in the Tonga-Kermadec region and their bearing on the depth extent of mantle flow, *J. Geophys. Res.*, **84**, 6783-6795.

RICHTER, F. M., and C. E. JOHNSON, 1974, Stability of a chemically layered mantle, *J. Geophys. Res.*, **79**, 1635-1639.

RICHTER, F. M., and D. P. MCKENZIE, 1981, On some consequences and possible causes of layered mantle convection, *J. Geophys. Res.*, **86**, 6133-6142.

RICHTER, F. M., and B. PARSONS, 1975, On the interaction of two scales of convection in the mantle, *J. Geophys. Res.*, **80**, 2529-2541.

ROACHE, P. J., 1978, Computational fluid dynamics, KOZOKEIKAKU Engineering Inc., **1**, pp. 309. (Japanese translation)

ROSSBY, H. T., 1969, A study of Benard convection with and without rotation, *J. Fluid Mech.*, **36**, 309-335.

SAMMIS, C. G., 1974, The effects of polymorphic phase boundaries on vertical and horizontal motions in the earth's mantle, *Tectonophysics*, **35**, 169-182.

SCLATER, J. G., C. JAUPART and D. GALSON, 1980, The heat flow through oceanic and continental crust and the heat loss of the earth, *Rev. Geophys. Space Phys.*, **18**, 269-311.

SHARPE, H. N., and W. R. PELTIER, 1979, A thermal history model for the earth with parameterized convection, *Geophys. J. R. astr. Soc.*, **59**, 191-203.

SMITH, K. A., 1966, On convective instability induced by surface-tension gradients, *J. Fluid Mech.*, **24**, 401-414.

TURCOTTE, D. L., and E. R. OXBURGH, 1969, Finite amplitude convection cells and continental drift, *J. Fluid Mech.*, 28, 29-42.

UKAJI, K., and R. SAWADA, 1970a, Celluar convection in the two layered fluids, *Abstracts*, The Meteological Society of Japan, **17**, 96. (in Japanese)

UKAJI, K., and R. SAWADA, 1970b, Celluar convection in the two layered fluids (2), *Abstracts*, The Meteological Society of Japan, **18**, 19. (in Japanense)

UKAJI, K., and R. SAWADA, 1971, Celluar convection in the two layered fluids (3), *Abstracts*, The Meteological Society of Japan, **25**, 21. (in Japanese)

YOKOKURA, T., 1979, Viscosity of the Earth's Mantle: Inference from Dynamic Support of Descending Slabs and Other Geophysical Evidence, Ph. D. Thesis, University of Tokyo, Tokyo, pp. 180.

ZEREN, R. W., and W. C. REYNOLDS, 1972, Thermal instabilities in two-fluid horizontal layers, *J. Fluid Mech.*, **53**, 305-327.

---

14. 層をなす対流の数値解析
—無限小および有限振幅の解析—

地震研究所　本多　了

最近，地球内部において，対流が半径方向に層をなしている可能性が指摘されている．本研究では，対流が層をなすことにより，どのような物理的結果が得られるかという点について，無限小振幅および有限振幅の数値解析をおこなった．

無限小振幅の解析においては，層をなす対流に二種類のモードかあることがわかった．一つは，流れが二種類の流体の境界面に対して反対称的なモードであり，もう一つは，境界面に対して対称的なモードである．これらのモードについては，すでに宇加治と沢田によって簡単な場合について報告されている．彼らの命名に従がえば，前者は thermal coupling であり，後者は mechanical coupling である．しかし，thermal coupling は，ごく特殊な場合においてのみ生ずるようである．また，mechanical coupling に比較して，より高次のモードと思われる．得られた stability curve の一部は，それぞれの層での stability を独立に考えることによって得られるそれと大体一致する．

有限振幅の計算においては，二次元の非圧縮で Prandtl 数が無限である流体を仮定し，Boussinesq 近似を用いて差分法により流れの場を求めた．Rayleigh 数が大となるにつれて，熱境界層が，流体の上面，下面および，二種類の流体の境界面に形成される．熱効率は，各層で定義される局所的な Rayleigh 数および Nusseldt 数の関係が，一層の場合のそれと同じであると考えることによって説明される．得られた解は全て mechanical coupling であった．
